PHYSICAL REVIEW D **108,** L031106 (2023)

Letter

Editors' Suggestion

Tests of *CP* symmetry in entangled $\Xi^0 - \bar{\Xi}^0$ pairs

M. Ablikim,[1] M. N. Achasov,[5,b] P. Adlarson,[75] X. C. Ai,[81] R. Aliberti,[36] A. Amoroso,[74a,74c] M. R. An,[40] Q. An,[71,58] Y. Bai,[57]
O. Bakina,[37] I. Balossino,[30a] Y. Ban,[47,g] V. Batozskaya,[1,45] K. Begzsuren,[33] N. Berger,[36] M. Berlowski,[45] M. Bertani,[29a]
D. Bettoni,[30a] F. Bianchi,[74a,74c] E. Bianco,[74a,74c] A. Bortone,[74a,74c] I. Boyko,[37] R. A. Briere,[6] A. Brueggemann,[68] H. Cai,[76]
X. Cai,[1,58] A. Calcaterra,[29a] G. F. Cao,[1,63] N. Cao,[1,63] S. A. Cetin,[62a] J. F. Chang,[1,58] T. T. Chang,[77] W. L. Chang,[1,63]
G. R. Che,[44] G. Chelkov,[37,a] C. Chen,[44] Chao Chen,[55] G. Chen,[1] H. S. Chen,[1,63] M. L. Chen,[1,58,63] S. J. Chen,[43]
S. M. Chen,[61] T. Chen,[1,63] X. R. Chen,[32,63] X. T. Chen,[1,63] Y. B. Chen,[1,58] Y. Q. Chen,[35] Z. J. Chen,[26,h] W. S. Cheng,[74c]
S. K. Choi,[11] X. Chu,[44] G. Cibinetto,[30a] S. C. Coen,[4] F. Cossio,[74c] J. J. Cui,[50] H. L. Dai,[1,58] J. P. Dai,[79] A. Dbeyssi,[19]
R. E. de Boer,[4] D. Dedovich,[37] Z. Y. Deng,[1] A. Denig,[36] I. Denysenko,[37] M. Destefanis,[74a,74c] F. De Mori,[74a,74c] B. Ding,[66,1]
X. X. Ding,[47,g] Y. Ding,[35] Y. Ding,[41] J. Dong,[1,58] L. Y. Dong,[1,63] M. Y. Dong,[1,58,63] X. Dong,[76] M. C. Du,[1] S. X. Du,[81]
Z. H. Duan,[43] P. Egorov,[37,a] Y. L. Fan,[76] J. Fang,[1,58] S. S. Fang,[1,63] W. X. Fang,[1] Y. Fang,[1] R. Farinelli,[30a] L. Fava,[74b,74c]
F. Feldbauer,[4] G. Felici,[29a] C. Q. Feng,[71,58] J. H. Feng,[59] K Fischer,[69] M. Fritsch,[4] C. Fritzsch,[68] C. D. Fu,[1] J. L. Fu,[63]
Y. W. Fu,[1] H. Gao,[63] Y. N. Gao,[47,g] Yang Gao,[71,58] S. Garbolino,[74c] I. Garzia,[30a,30b] P. T. Ge,[76] Z. W. Ge,[43] C. Geng,[59]
E. M. Gersabeck,[67] A Gilman,[69] K. Goetzen,[14] L. Gong,[41] W. X. Gong,[1,58] W. Gradl,[36] S. Gramigna,[30a,30b] M. Greco,[74a,74c]
M. H. Gu,[1,58] Y. T. Gu,[16] C. Y Guan,[1,63] Z. L. Guan,[23] A. Q. Guo,[32,63] L. B. Guo,[42] M. J. Guo,[50] R. P. Guo,[49] Y. P. Guo,[13,f]
A. Guskov,[37,a] T. T. Han,[50] W. Y. Han,[40] X. Q. Hao,[20] F. A. Harris,[65] K. K. He,[55] K. L. He,[1,63] F. H H. Heinsius,[4]
C. H. Heinz,[36] Y. K. Heng,[1,58,63] C. Herold,[60] T. Holtmann,[4] P. C. Hong,[13,f] G. Y. Hou,[1,63] X. T. Hou,[1,63] Y. R. Hou,[63]
Z. L. Hou,[1] H. M. Hu,[1,63] J. F. Hu,[56,i] T. Hu,[1,58,63] Y. Hu,[1] G. S. Huang,[71,58] K. X. Huang,[59] L. Q. Huang,[32,63] X. T. Huang,[50]
Y. P. Huang,[1] T. Hussain,[73] N Hüsken,[28,36] W. Imoehl,[28] M. Irshad,[71,58] J. Jackson,[28] S. Jaeger,[4] S. Janchiv,[33] J. H. Jeong,[11]
Q. Ji,[1] Q. P. Ji,[20] X. B. Ji,[1,63] X. L. Ji,[1,58] Y. Y. Ji,[50] X. Q. Jia,[50] Z. K. Jia,[71,58] P. C. Jiang,[47,g] S. S. Jiang,[40] T. J. Jiang,[17]
X. S. Jiang,[1,58,63] Y. Jiang,[63] J. B. Jiao,[50] Z. Jiao,[24] S. Jin,[43] Y. Jin,[66] M. Q. Jing,[1,63] T. Johansson,[75] X. K.,[1] S. Kabana,[34]
N. Kalantar-Nayestanaki,[64] X. L. Kang,[10] X. S. Kang,[41] R. Kappert,[64] M. Kavatsyuk,[64] B. C. Ke,[81] A. Khoukaz,[68]
R. Kiuchi,[1] R. Kliemt,[14] O. B. Kolcu,[62a] B. Kopf,[4] M. K. Kuessner,[4] A. Kupsc,[45,75] W. Kühn,[38] J. J. Lane,[67] P. Larin,[19]
A. Lavania,[27] L. Lavezzi,[74a,74c] T. T. Lei,[71,k] Z. H. Lei,[71,58] H. Leithoff,[36] M. Lellmann,[36] T. Lenz,[36] C. Li,[48] C. Li,[44]
C. H. Li,[40] Cheng Li,[71,58] D. M. Li,[81] F. Li,[1,58] G. Li,[1] H. Li,[71,58] H. B. Li,[1,63] H. J. Li,[20] H. N. Li,[56,i] Hui Li,[44] J. R. Li,[61]
J. S. Li,[59] J. W. Li,[50] K. L. Li,[20] Ke Li,[1] L. J Li,[1,63] L. K. Li,[1] Lei Li,[3] M. H. Li,[44] P. R. Li,[39,j,k] Q. X. Li,[50] S. X. Li,[13] T. Li,[50]
W. D. Li,[1,63] W. G. Li,[1] X. H. Li,[71,58] X. L. Li,[50] Xiaoyu Li,[1,63] Y. G. Li,[47,g] Z. J. Li,[59] Z. X. Li,[16] C. Liang,[43] H. Liang,[1,63]
H. Liang,[71,58] H. Liang,[35] Y. F. Liang,[54] Y. T. Liang,[32,63] G. R. Liao,[15] L. Z. Liao,[50] J. Libby,[27] A. Limphirat,[60] D. X. Lin,[32,63]
T. Lin,[1] B. J. Liu,[1] B. X. Liu,[76] C. Liu,[35] C. X. Liu,[1] F. H. Liu,[53] Fang Liu,[1] Feng Liu,[7] G. M. Liu,[56,i] H. Liu,[39,j,k] H. B. Liu,[16]
H. M. Liu,[1,63] Huanhuan Liu,[1] Huihui Liu,[22] J. B. Liu,[71,58] J. L. Liu,[72] J. Y. Liu,[1,63] K. Liu,[1] K. Y. Liu,[41] Ke Liu,[23] L. Liu,[71,58]
L. C. Liu,[44] Lu Liu,[44] M. H. Liu,[13,f] P. L. Liu,[1] Q. Liu,[63] S. B. Liu,[71,58] T. Liu,[13,f] W. K. Liu,[44] W. M. Liu,[71,58] X. Liu,[39,j,k]
Y. Liu,[81] Y. Liu,[39,j,k] Y. B. Liu,[44] Z. A. Liu,[1,58,63] Z. Q. Liu,[50] X. C. Lou,[1,58,63] F. X. Lu,[59] H. J. Lu,[24] J. G. Lu,[1,58] X. L. Lu,[1]
Y. Lu,[8] Y. P. Lu,[1,58] Z. H. Lu,[1,63] C. L. Luo,[42] M. X. Luo,[80] T. Luo,[13,f] X. L. Luo,[1,58] X. R. Lyu,[63] Y. F. Lyu,[44] F. C. Ma,[41]
H. L. Ma,[1] J. L. Ma,[1,63] L. L. Ma,[50] M. M. Ma,[1,63] Q. M. Ma,[1] R. Q. Ma,[1,63] R. T. Ma,[63] X. Y. Ma,[1,58] Y. Ma,[47,g] Y. M. Ma,[32]
F. E. Maas,[19] M. Maggiora,[74a,74c] S. Malde,[69] Q. A. Malik,[73] A. Mangoni,[29b] Y. J. Mao,[47,g] Z. P. Mao,[1] S. Marcello,[74a,74c]
Z. X. Meng,[66] J. G. Messchendorp,[14,64] G. Mezzadri,[30a] H. Miao,[1,63] T. J. Min,[43] R. E. Mitchell,[28] X. H. Mo,[1,58,63]
N. Yu. Muchnoi,[5,b] Y. Nefedov,[37] F. Nerling,[19,d] I. B. Nikolaev,[5,b] Z. Ning,[1,58] S. Nisar,[12,l] Y. Niu,[50] S. L. Olsen,[63]
Q. Ouyang,[1,58,63] S. Pacetti,[29b,29c] X. Pan,[55] Y. Pan,[57] A. Pathak,[35] P. Patteri,[29a] Y. P. Pei,[71,58] M. Pelizaeus,[4] H. P. Peng,[71,58]
K. Peters,[14,d] J. L. Ping,[42] R. G. Ping,[1,63] S. Plura,[36] S. Pogodin,[37] V. Prasad,[34] F. Z. Qi,[1] H. Qi,[71,58] H. R. Qi,[61] M. Qi,[43]
T. Y. Qi,[13,f] S. Qian,[1,58] W. B. Qian,[63] C. F. Qiao,[63] J. J. Qin,[72] L. Q. Qin,[15] X. P. Qin,[13,f] X. S. Qin,[50] Z. H. Qin,[1,58] J. F. Qiu,[1]
S. Q. Qu,[61] C. F. Redmer,[36] K. J. Ren,[40] A. Rivetti,[74c] V. Rodin,[64] M. Rolo,[74c] G. Rong,[1,63] Ch. Rosner,[19] S. N. Ruan,[44]
N. Salone,[45] A. Sarantsev,[37,c] Y. Schelhaas,[36] K. Schoenning,[75] M. Scodeggio,[30a,30b] K. Y. Shan,[13,f] W. Shan,[25]
X. Y. Shan,[71,58] J. F. Shangguan,[55] L. G. Shao,[1,63] M. Shao,[71,58] C. P. Shen,[13,f] H. F. Shen,[1,63] W. H. Shen,[63] X. Y. Shen,[1,63]
B. A. Shi,[63] H. C. Shi,[71,58] J. L. Shi,[13] J. Y. Shi,[1] Q. Q. Shi,[55] R. S. Shi,[1,63] X. Shi,[1,58] J. J. Song,[20] T. Z. Song,[59]
W. M. Song,[35,1] Y. J. Song,[13] Y. X. Song,[47,g] S. Sosio,[74a,74c] S. Spataro,[74a,74c] F. Stieler,[36] Y. J. Su,[63] G. B. Sun,[76] G. X. Sun,[1]
H. Sun,[63] H. K. Sun,[1] J. F. Sun,[20] K. Sun,[61] L. Sun,[76] S. S. Sun,[1,63] T. Sun,[1,63] W. Y. Sun,[35] Y. Sun,[10] Y. J. Sun,[71,58]
Y. Z. Sun,[1] Z. T. Sun,[50] Y. X. Tan,[71,58] C. J. Tang,[54] G. Y. Tang,[1] J. Tang,[59] Y. A. Tang,[76] L. Y Tao,[72] Q. T. Tao,[26,h] M. Tat,[69]
J. X. Teng,[71,58] V. Thoren,[75] W. H. Tian,[52] W. H. Tian,[59] Y. Tian,[32,63] Z. F. Tian,[76] I. Uman,[62b] S. J. Wang,[50] B. Wang,[1]
B. L. Wang,[63] Bo Wang,[71,58] C. W. Wang,[43] D. Y. Wang,[47,g] F. Wang,[72] H. J. Wang,[39,j,k] H. P. Wang,[1,63] J. P. Wang,[50]
K. Wang,[1,58] L. L. Wang,[1] M. Wang,[50] Meng Wang,[1,63] S. Wang,[39,j,k] S. Wang,[13,f] T. Wang,[13,f] T. J. Wang,[44] W. Wang,[59]
W. Wang,[72] W. P. Wang,[71,58] X. Wang,[47,g] X. F. Wang,[39,j,k] X. J. Wang,[40] X. L. Wang,[13,f] Y. Wang,[61] Y. D. Wang,[46]

2470-0010/2023/108(3)/L031106(10)

Published by the American Physical Society

Y. F. Wang,[1,58,63] Y. H. Wang,[48] Y. N. Wang,[46] Y. Q. Wang,[1] Yaqian Wang,[18,1] Yi Wang,[61] Z. Wang,[1,58] Z. L. Wang,[72]
Z. Y. Wang,[1,63] Ziyi Wang,[63] D. Wei,[70] D. H. Wei,[15] F. Weidner,[68] S. P. Wen,[1] C. W. Wenzel,[4] U. W. Wiedner,[4]
G. Wilkinson,[69] M. Wolke,[75] L. Wollenberg,[4] C. Wu,[40] J. F. Wu,[1,63] L. H. Wu,[1] L. J. Wu,[1,63] X. Wu,[13,f] X. H. Wu,[35] Y. Wu,[71]
Y. J. Wu,[32] Z. Wu,[1,58] L. Xia,[71,58] X. M. Xian,[40] T. Xiang,[47,g] D. Xiao,[39,j,k] G. Y. Xiao,[43] H. Xiao,[13,f] S. Y. Xiao,[1]
Y. L. Xiao,[13,f] Z. J. Xiao,[42] C. Xie,[43] X. H. Xie,[47,g] Y. Xie,[50] Y. G. Xie,[1,58] Y. H. Xie,[7] Z. P. Xie,[71,58] T. Y. Xing,[1,63]
C. F. Xu,[1,63] C. J. Xu,[59] G. F. Xu,[1] H. Y. Xu,[66] Q. J. Xu,[17] Q. N. Xu,[31] W. Xu,[1,63] W. L. Xu,[66] X. P. Xu,[55] Y. C. Xu,[78]
Z. P. Xu,[43] Z. S. Xu,[63] F. Yan,[13,f] L. Yan,[13,f] W. B. Yan,[71,58] W. C. Yan,[81] X. Q. Yan,[1] H. J. Yang,[51,e] H. L. Yang,[35]
H. X. Yang,[1] Tao Yang,[1] Y. Yang,[13,f] Y. F. Yang,[44] Y. X. Yang,[1,63] Yifan Yang,[1,63] Z. W. Yang,[39,j,k] Z. P. Yao,[50] M. Ye,[1,58]
M. H. Ye,[9] J. H. Yin,[1] Z. Y. You,[59] B. X. Yu,[1,58,63] C. X. Yu,[44] G. Yu,[1,63] J. S. Yu,[26,h] T. Yu,[72] X. D. Yu,[47,g] C. Z. Yuan,[1,63]
L. Yuan,[2] S. C. Yuan,[1] X. Q. Yuan,[1] Y. Yuan,[1,63] Z. Y. Yuan,[59] C. X. Yue,[40] A. A. Zafar,[73] F. R. Zeng,[50] X. Zeng,[13,f]
Y. Zeng,[26,h] Y. J. Zeng,[1,63] X. Y. Zhai,[35] Y. C. Zhai,[50] Y. H. Zhan,[59] A. Q. Zhang,[1,63] B. L. Zhang,[1,63] B. X. Zhang,[1]
D. H. Zhang,[44] G. Y. Zhang,[20] H. Zhang,[71] H. H. Zhang,[35] H. H. Zhang,[59] H. Q. Zhang,[1,58,63] H. Y. Zhang,[1,58] J. J. Zhang,[52]
J. L. Zhang,[21] J. Q. Zhang,[42] J. W. Zhang,[1,58,63] J. X. Zhang,[39,j,k] J. Y. Zhang,[1] J. Z. Zhang,[1,63] Jianyu Zhang,[63]
Jiawei Zhang,[1,63] L. M. Zhang,[61] L. Q. Zhang,[59] Lei Zhang,[43] P. Zhang,[1] Q. Y. Zhang,[40,81] Shuihan Zhang,[1,63]
Shulei Zhang,[26,h] X. D. Zhang,[46] X. M. Zhang,[1] X. Y. Zhang,[55] X. Y. Zhang,[50] Y. Zhang,[72] Y. Zhang,[69] Y. T. Zhang,[81]
Y. H. Zhang,[1,58] Yan Zhang,[71,58] Yao Zhang,[1] Z. H. Zhang,[1] Z. L. Zhang,[35] Z. Y. Zhang,[76] Z. Y. Zhang,[44] G. Zhao,[1]
J. Zhao,[40] J. Y. Zhao,[1,63] J. Z. Zhao,[1,58] Lei Zhao,[71,58] Ling Zhao,[1] M. G. Zhao,[44] S. J. Zhao,[81] Y. B. Zhao,[1,58] Y. X. Zhao,[32,63]
Z. G. Zhao,[71,58] A. Zhemchugov,[37,a] B. Zheng,[72] J. P. Zheng,[1,58] W. J. Zheng,[1,63] Y. H. Zheng,[63] B. Zhong,[42] X. Zhong,[59]
H. Zhou,[50] L. P. Zhou,[1,63] X. Zhou,[76] X. K. Zhou,[7] X. R. Zhou,[71,58] X. Y. Zhou,[40] Y. Z. Zhou,[13,f] J. Zhu,[44] K. Zhu,[1]
K. J. Zhu,[1,58,63] L. Zhu,[35] L. X. Zhu,[63] S. H. Zhu,[70] S. Q. Zhu,[43] T. J. Zhu,[13,f] W. J. Zhu,[13,f] Y. C. Zhu,[71,58] Z. A. Zhu,[1,63]
J. H. Zou,[1] and J. Zu[71,58]

(BESIII Collaboration)

[1]*Institute of High Energy Physics, Beijing 100049, People's Republic of China*
[2]*Beihang University, Beijing 100191, People's Republic of China*
[3]*Beijing Institute of Petrochemical Technology, Beijing 102617, People's Republic of China*
[4]*Bochum Ruhr-University, D-44780 Bochum, Germany*
[5]*Budker Institute of Nuclear Physics SB RAS (BINP), Novosibirsk 630090, Russia*
[6]*Carnegie Mellon University, Pittsburgh, Pennsylvania 15213, USA*
[7]*Central China Normal University, Wuhan 430079, People's Republic of China*
[8]*Central South University, Changsha 410083, People's Republic of China*
[9]*China Center of Advanced Science and Technology, Beijing 100190, People's Republic of China*
[10]*China University of Geosciences, Wuhan 430074, People's Republic of China*
[11]*Chung-Ang University, Seoul 06974, Republic of Korea*
[12]*COMSATS University Islamabad, Lahore Campus,*
Defence Road, Off Raiwind Road, 54000 Lahore, Pakistan
[13]*Fudan University, Shanghai 200433, People's Republic of China*
[14]*GSI Helmholtzcentre for Heavy Ion Research GmbH, D-64291 Darmstadt, Germany*
[15]*Guangxi Normal University, Guilin 541004, People's Republic of China*
[16]*Guangxi University, Nanning 530004, People's Republic of China*
[17]*Hangzhou Normal University, Hangzhou 310036, People's Republic of China*
[18]*Hebei University, Baoding 071002, People's Republic of China*
[19]*Helmholtz Institute Mainz, Staudinger Weg 18, D-55099 Mainz, Germany*
[20]*Henan Normal University, Xinxiang 453007, People's Republic of China*
[21]*Henan University, Kaifeng 475004, People's Republic of China*
[22]*Henan University of Science and Technology, Luoyang 471003, People's Republic of China*
[23]*Henan University of Technology, Zhengzhou 450001, People's Republic of China*
[24]*Huangshan College, Huangshan 245000, People's Republic of China*
[25]*Hunan Normal University, Changsha 410081, People's Republic of China*
[26]*Hunan University, Changsha 410082, People's Republic of China*
[27]*Indian Institute of Technology Madras, Chennai 600036, India*
[28]*Indiana University, Bloomington, Indiana 47405, USA*
[29a]*INFN Laboratori Nazionali di Frascati, INFN Laboratori Nazionali di Frascati, I-00044, Frascati, Italy*
[29b]*INFN Laboratori Nazionali di Frascati, INFN Sezione di Perugia, I-06100, Perugia, Italy*
[29c]*INFN Laboratori Nazionali di Frascati, University of Perugia, I-06100, Perugia, Italy*

[30a]*INFN Sezione di Ferrara, INFN Sezione di Ferrara, I-44122, Ferrara, Italy*
[30b]*INFN Sezione di Ferrara, University of Ferrara, I-44122, Ferrara, Italy*
[31]*Inner Mongolia University, Hohhot 010021, People's Republic of China*
[32]*Institute of Modern Physics, Lanzhou 730000, People's Republic of China*
[33]*Institute of Physics and Technology, Peace Avenue 54B, Ulaanbaatar 13330, Mongolia*
[34]*Instituto de Alta Investigación, Universidad de Tarapacá, Casilla 7D, Arica 1000000, Chile*
[35]*Jilin University, Changchun 130012, People's Republic of China*
[36]*Johannes Gutenberg University of Mainz,*
Johann-Joachim-Becher-Weg 45, D-55099 Mainz, Germany
[37]*Joint Institute for Nuclear Research, 141980 Dubna, Moscow region, Russia*
[38]*Justus-Liebig-Universitaet Giessen, II. Physikalisches Institut,*
Heinrich-Buff-Ring 16, D-35392 Giessen, Germany
[39]*Lanzhou University, Lanzhou 730000, People's Republic of China*
[40]*Liaoning Normal University, Dalian 116029, People's Republic of China*
[41]*Liaoning University, Shenyang 110036, People's Republic of China*
[42]*Nanjing Normal University, Nanjing 210023, People's Republic of China*
[43]*Nanjing University, Nanjing 210093, People's Republic of China*
[44]*Nankai University, Tianjin 300071, People's Republic of China*
[45]*National Centre for Nuclear Research, Warsaw 02-093, Poland*
[46]*North China Electric Power University, Beijing 102206, People's Republic of China*
[47]*Peking University, Beijing 100871, People's Republic of China*
[48]*Qufu Normal University, Qufu 273165, People's Republic of China*
[49]*Shandong Normal University, Jinan 250014, People's Republic of China*
[50]*Shandong University, Jinan 250100, People's Republic of China*
[51]*Shanghai Jiao Tong University, Shanghai 200240, People's Republic of China*
[52]*Shanxi Normal University, Linfen 041004, People's Republic of China*
[53]*Shanxi University, Taiyuan 030006, People's Republic of China*
[54]*Sichuan University, Chengdu 610064, People's Republic of China*
[55]*Soochow University, Suzhou 215006, People's Republic of China*
[56]*South China Normal University, Guangzhou 510006, People's Republic of China*
[57]*Southeast University, Nanjing 211100, People's Republic of China*
[58]*State Key Laboratory of Particle Detection and Electronics,*
Beijing 100049, Hefei 230026, People's Republic of China
[59]*Sun Yat-Sen University, Guangzhou 510275, People's Republic of China*
[60]*Suranaree University of Technology, University Avenue 111, Nakhon Ratchasima 30000, Thailand*
[61]*Tsinghua University, Beijing 100084, People's Republic of China*
[62a]*Turkish Accelerator Center Particle Factory Group, Istinye University, 34010, Istanbul, Turkey*
[62b]*Turkish Accelerator Center Particle Factory Group, Near East University,*
Nicosia, North Cyprus, 99138, Mersin 10, Turkey
[63]*University of Chinese Academy of Sciences, Beijing 100049, People's Republic of China*
[64]*University of Groningen, NL-9747 AA Groningen, The Netherlands*
[65]*University of Hawaii, Honolulu, Hawaii 96822, USA*
[66]*University of Jinan, Jinan 250022, People's Republic of China*
[67]*University of Manchester, Oxford Road, Manchester, M13 9PL, United Kingdom*
[68]*University of Muenster, Wilhelm-Klemm-Strasse 9, 48149 Muenster, Germany*
[69]*University of Oxford, Keble Road, Oxford OX13RH, United Kingdom*
[70]*University of Science and Technology Liaoning, Anshan 114051, People's Republic of China*
[71]*University of Science and Technology of China, Hefei 230026, People's Republic of China*
[72]*University of South China, Hengyang 421001, People's Republic of China*
[73]*University of the Punjab, Lahore-54590, Pakistan*
[74a]*University of Turin and INFN, University of Turin, I-10125, Turin, Italy*
[74b]*University of Turin and INFN, University of Eastern Piedmont, I-15121, Alessandria, Italy*
[74c]*University of Turin and INFN, INFN, I-10125, Turin, Italy*
[75]*Uppsala University, Box 516, SE-75120 Uppsala, Sweden*
[76]*Wuhan University, Wuhan 430072, People's Republic of China*
[77]*Xinyang Normal University, Xinyang 464000, People's Republic of China*
[78]*Yantai University, Yantai 264005, People's Republic of China*
[79]*Yunnan University, Kunming 650500, People's Republic of China*

[80]*Zhejiang University, Hangzhou 310027, People's Republic of China*
[81]*Zhengzhou University, Zhengzhou 450001, People's Republic of China*

(Received 16 May 2023; revised 4 June 2023; accepted 20 July 2023; published 23 August 2023)

The $J/\psi \to \Xi^0\bar{\Xi}^0$ process and subsequent decays are investigated using $(10087 \pm 44) \times 10^6$ J/ψ events collected at the BESIII experiment. The decay parameters of Ξ^0 and $\bar{\Xi}^0$ are simultaneously measured to be $\alpha_\Xi = -0.3750 \pm 0.0034 \pm 0.0016$, $\bar{\alpha}_\Xi = 0.3790 \pm 0.0034 \pm 0.0021$, $\phi_\Xi = 0.0051 \pm 0.0096 \pm 0.0018$ rad, $\bar{\phi}_\Xi = -0.0053 \pm 0.0097 \pm 0.0019$ rad with unprecedented accuracies, where the first and the second uncertainties are statistical and systematic, respectively. The most precise values for CP asymmetry observables of Ξ^0 decay are obtained to be $A_{CP}^{\Xi} = (-5.4 \pm 6.5 \pm 3.1) \times 10^{-3}$ and $\Delta\phi_{CP}^{\Xi} = (-0.1 \pm 6.9 \pm 0.9) \times 10^{-3}$ rad. For the first time, the weak and strong phase differences are determined to be $\xi_P - \xi_S = (0.0 \pm 1.7 \pm 0.2) \times 10^{-2}$ rad and $\delta_P - \delta_S = (-1.3 \pm 1.7 \pm 0.4) \times 10^{-2}$ rad, which are the most precise results for any weakly decaying baryon. These results will play important roles in the studies of the CP violations and polarizations for the strange, charmed, and beauty baryons.

DOI: 10.1103/PhysRevD.108.L031106

At present, there is no satisfactory explanation for why our Universe is matter dominated. Following Sakharov [1], generation of a matter-antimatter imbalance requires the fulfillment of three criteria. One of these is the existence of processes that violate charge conjugation and parity (CP). Note that CP violation (CPV) is accommodated in the Standard Model of particle physics through the Cabbibo-Kobayashi-Maskawa (CKM) mechanism and is experimentally established in the meson sector [2–5]. However, the observed CPV in meson decays can only generate a matter-antimatter asymmetry that is 8 orders of magnitude smaller than that in our Universe [6,7]. The advent of high-intensity facilities producing hyperons and antihyperons in abundance opens up a new possibility: the search for CPV in hyperon decays [8–11].

Hyperon decays are valuable since they can provide a way to measure $\Delta S = 1$ CP nonconservation, which is complementary to kaon decays in which the $\Delta S = 2$ effects are dominant. The observed CPV from the $\Delta S = 2$ contributions in kaon decays can be well described by the CKM mechanism. However, in the CKM mechanism, $\Delta S = 1$ effects can also be produced through a penguin diagram [12,13], which generates a nonzero value of the kaon decay parameter ϵ'. The penguin diagram could produce CP-odd effects at order $20\epsilon'$ in hyperon decays; therefore, hyperons have more potential to discover these effects. The Weinberg-Higgs model [14,15] and left-right–symmetric model [16–18] also predict the $\Delta S = 1$ CPV. Therefore, it is crucial to search for CPV in hyperon decays, and it has been demonstrated in several measurements by the BESIII Collaboration, where analyses of polarized and entangled pairs of single-strange Λ [19,20] and Σ^+ [21] hyperons resulted in the most precise CP tests so far for baryons. Sequential decays of double-strange Ξ hyperons are more intriguing since they allow the separation of strong and weak phase differences, as demonstrated by the measurements of Ξ^- [22,23]. Its isospin partner, i.e., the Ξ^0 hyperon, provides independent measurements of the $s \to u$ transition and the weak and strong phase differences. In many previous experiments, the CP tests rely on the products of weak and strong phase differences. In this way, it is difficult to distinguish the contributions of weak

---

[a] Also at the Moscow Institute of Physics and Technology, Moscow 141700, Russia.

[b] Also at the Novosibirsk State University, Novosibirsk 630090, Russia.

[c] Also at the NRC "Kurchatov Institute," PNPI, Gatchina 188300, Russia.

[d] Also at Goethe University Frankfurt, 60323 Frankfurt am Main, Germany.

[e] Also at Key Laboratory for Particle Physics, Astrophysics and Cosmology, Ministry of Education; Shanghai Key Laboratory for Particle Physics and Cosmology; Institute of Nuclear and Particle Physics, Shanghai 200240, People's Republic of China.

[f] Also at Key Laboratory of Nuclear Physics and Ion-Beam Application (MOE) and Institute of Modern Physics, Fudan University, Shanghai 200443, People's Republic of China.

[g] Also at State Key Laboratory of Nuclear Physics and Technology, Peking University, Beijing 100871, People's Republic of China.

[h] Also at School of Physics and Electronics, Hunan University, Changsha 410082, China.

[i] Also at Guangdong Provincial Key Laboratory of Nuclear Science, Institute of Quantum Matter, South China Normal University, Guangzhou 510006, China.

[j] Also at Frontiers Science Center for Rare Isotopes, Lanzhou University, Lanzhou 730000, People's Republic of China.

[k] Also at Lanzhou Center for Theoretical Physics, Lanzhou University, Lanzhou 730000, People's Republic of China.

[l] Also at the Department of Mathematical Sciences, IBA, Karachi 75270, Pakistan.

interactions from that of strong interactions. In Ξ hyperon sequential decays, the separation of weak and strong phase differences allows us to directly determine the *CPV* sources from the Standard Model and beyond [9,24].

The decay amplitude of a spin-1/2 hyperon into a lighter spin-1/2 baryon and a pseudoscalar meson has a parity-violating S-wave component and a parity-conserving P-wave component. Hence, it can be completely described by the two independent decay parameters α and ϕ [8,9,25]. The decay parameters $\alpha_\Xi(\alpha_\Lambda), \phi_\Xi, \bar{\alpha}_\Xi(\bar{\alpha}_\Lambda), \bar{\phi}_\Xi$ of $\Xi^0(\Lambda)$ and $\bar{\Xi}^0(\bar{\Lambda})$ hyperons can be determined from the sequential decays $\Xi^0 \to \Lambda(\to p\pi^-)\pi^0$ and $\bar{\Xi}^0 \to \bar{\Lambda}(\to \bar{p}\pi^+)\pi^0$. Precise measurements of the Ξ^0 decay parameters are important for studies of spin polarization and decay parameters of many other baryon ($\Omega^-, \Lambda_c, \Xi_c, \Xi_b$, etc.) decays into final states involving Ξ^0 [26–28].

In this Letter, we present measurements of Ξ^0 and $\bar{\Xi}^0$ decay parameters and *CP* asymmetries with a nine-dimensional fit to the full angular distributions of the quantum-entangled $\Xi^0 - \bar{\Xi}^0$ sequential decays.

Three *CP* asymmetry observables A_{CP}^{Ξ}, $\Delta\phi_{CP}^{\Xi}$, and A_{CP}^{Λ} are defined by the following equations:

$$A_{CP}^{\Xi} = (\alpha_\Xi + \bar{\alpha}_\Xi)/(\alpha_\Xi - \bar{\alpha}_\Xi), \tag{1}$$

$$\Delta\phi_{CP}^{\Xi} = (\phi_\Xi + \bar{\phi}_\Xi)/2, \tag{2}$$

$$A_{CP}^{\Lambda} = (\alpha_\Lambda + \bar{\alpha}_\Lambda)/(\alpha_\Lambda - \bar{\alpha}_\Lambda), \tag{3}$$

since *CP* conservation implies $\alpha_\Xi = -\bar{\alpha}_\Xi$, $\phi_\Xi = -\bar{\phi}_\Xi$, and $\alpha_\Lambda = -\bar{\alpha}_\Lambda$. According to Ref. [10], A_{CP}^{Ξ} is proportional to the product of the weak phase difference $(\xi_P - \xi_S)$ and the strong phase difference $(\delta_P - \delta_S)$ of the final state interaction. Hence, for the case of a tiny strong phase difference, A_{CP}^{Ξ} would vanish even if the weak phase difference is nonzero. However, $\Delta\phi_{CP}^{\Xi}$ does not have this problem [10] and is more sensitive than A_{CP}^{Ξ} for detecting *CPV*. The weak and strong phase differences can be determined from [9,24]

$$\tan(\xi_P - \xi_S) = \frac{\sqrt{1-\alpha_\Xi^2}\sin\phi_\Xi + \sqrt{1-\bar{\alpha}_\Xi^2}\sin\bar{\phi}_\Xi}{\alpha_\Xi - \bar{\alpha}_\Xi}, \tag{4}$$

$$\tan(\delta_P - \delta_S) = \frac{\sqrt{1-\alpha_\Xi^2}\sin\phi_\Xi - \sqrt{1-\bar{\alpha}_\Xi^2}\sin\bar{\phi}_\Xi}{\alpha_\Xi - \bar{\alpha}_\Xi}. \tag{5}$$

This analysis is based on the sample of $(10087 \pm 44) \times 10^6$ J/ψ events [29] collected with the BESIII detector at the BEPCII collider. Details about BEPCII and BESIII can be found in Refs. [30–33]. A J/ψ Monte Carlo (MC) simulation is used to determine the detector efficiency, optimize the event selection, and estimate the background. The simulation is performed by GEANT4-based [34] software [35], which includes the geometric description of the BESIII detector and the detector response. The simulation models the beam energy spread and initial state radiation (ISR) in the e^+e^- annihilations with the generator KKMC [36]. The known decay modes of J/ψ are modeled with EvtGen [37], and the remaining unknown decays are modeled with LUNDCHARM [38]. For the signal process, $J/\psi \to \Xi^0\bar{\Xi}^0$, $\Xi^0 \to \Lambda(\to p\pi^-)\pi^0$, $\bar{\Xi}^0 \to \bar{\Lambda}(\to \bar{p}\pi^+)\pi^0$, $\pi^0 \to \gamma\gamma$, two different MC samples are used. One is generated according to a phase space model (PHSP MC) for determination of the parameters, and the other is generated according to the joint angular distribution with the parameters obtained by this analysis (signal MC).

The Λ and $\bar{\Lambda}$ hyperons are reconstructed from their dominant hadronic decay mode, $\Lambda(\bar{\Lambda}) \to p\pi^-(\bar{p}\pi^+)$. The charged tracks are detected in the multilayer drift chamber (MDC) under the requirement that $|\cos\theta| < 0.93$, where θ is the angle between the momentum of the charged track and the axis of the detector. Events with at least four charged tracks are retained. Tracks with momentum larger than 0.3 GeV/c are considered as proton candidates, and otherwise as pion candidates. There are no further particle identification requirements. Vertex fits [39] are performed using all combinations with oppositely charged proton and pion candidates, constraining them to a common vertex. The combinations which pass the vertex fit and have invariant masses within the range $[1.111, 1.120]$ GeV/c^2 are regarded as Λ and $\bar{\Lambda}$ candidates.

The photons used for reconstructing the π^0 candidates are detected in the electromagnetic calorimeter (EMC). Each photon is required to have an EMC energy deposit of more than 25 MeV in the barrel region ($|\cos\theta| < 0.80$) or more than 50 MeV in the end-cap region ($0.86 < |\cos\theta| < 0.92$). To suppress electronic noise and showers unrelated to the event, the difference between the EMC time and the event start time is required to be within (0, 700) ns. The π^0 candidates require at least one photon to come from the barrel region and invariant mass within the range $[0.098, 0.165]$ GeV/c^2. A kinematic fit [40] constraining the $\gamma\gamma$ invariant mass to the known π^0 mass [41] is performed, and the resulting χ^2 must be smaller than 200.

Events with at least one Λ candidate, one $\bar{\Lambda}$ candidate, and two π^0 candidates are considered for further analysis. A four-constraint (4C) kinematic fit is performed on the $\Lambda\bar{\Lambda}\pi^0\pi^0$ hypothesis, constraining the total reconstructed four-momentum to that of the initial J/ψ. If there is more than one combination of $\Lambda\bar{\Lambda}\pi^0\pi^0$, the one with the smallest χ^2 of the 4C fit (χ^2_{4C}) is selected, and $\chi^2_{4C} < 100$ is required. Since there are two π^0 candidates (π^0_1, π^0_2) per event, there will be two possible combinations of $\Lambda(\bar{\Lambda})$ and π^0. The combination which minimizes the quantity $(m_{\Lambda\pi^0_1} - M_{\Xi^0})^2 + (m_{\bar{\Lambda}\pi^0_2} - M_{\Xi^0})^2$ is kept, where $m_{\Lambda\pi^0_1}$ and $m_{\bar{\Lambda}\pi^0_2}$ are the invariant masses of $\Lambda\pi^0_1$ and $\bar{\Lambda}\pi^0_2$, respectively, and M_{Ξ^0} is the known mass of Ξ^0 [41]. The requirements suppress

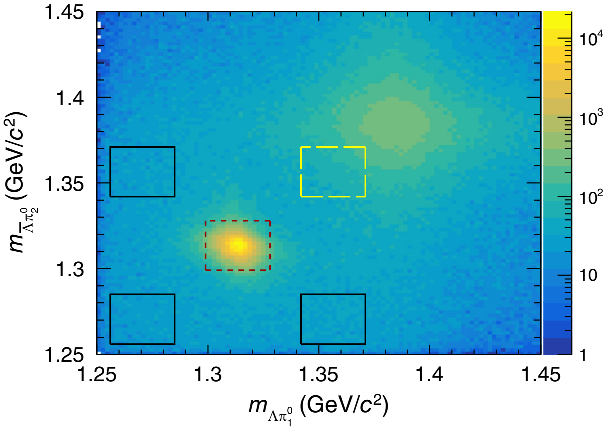

FIG. 1. Distribution of $m_{\Lambda\pi_1^0}$ versus $m_{\bar{\Lambda}\pi_2^0}$, where the red short-dashed-line box indicates the signal region, and the black and yellow long-dashed-line boxes are the sideband regions.

the amount of miscombinations to approximately 0.7%. To reduce background from sources with the same final states, e.g., $J/\psi \to \Sigma^0(1385)\bar{\Sigma}^0(1385), \Sigma^0(1385) \to \Lambda(\to p\pi^-)\pi^0$, $\bar{\Sigma}^0(1385) \to \bar{\Lambda}(\to \bar{p}\pi^+)\pi^0$, $\pi^0 \to \gamma\gamma$, the $m_{\Lambda\pi_1^0}$ and $m_{\bar{\Lambda}\pi_2^0}$ are required to be within $[1.299, 1.328]$ GeV/c^2. Figure 1 shows the two-dimensional distribution of the reconstructed $\bar{\Xi}^0$ mass versus the reconstructed Ξ^0 mass. After applying all the event selection criteria, we obtain a sample of 327,305 events.

An inclusive MC sample of 10 billion J/ψ events is used for studying potential backgrounds. After applying the same selection criteria as for data, the main background contribution is found to be from the decay $J/\psi \to \Sigma^0(1385)\bar{\Sigma}^0(1385)$. A dedicated simulation of the process $J/\psi \to \Sigma^0(1385)\bar{\Sigma}^0(1385)$ according to the measured angular distribution by Ref. [42] is carried out, and the corresponding number of background events from this channel in data is estimated to be 1697 ± 139. All other background contributions are estimated from the sideband regions of the two-dimensional distribution of $m_{\Lambda\pi_1^0}$ versus $m_{\bar{\Lambda}\pi_2^0}$. The sideband regions are defined by $|m_{\Lambda\pi^0}(m_{\bar{\Lambda}\pi^0}) - M_{\Xi^0}| \in [0.0285, 0.0575]$ GeV/c^2 and shown as black and yellow long-dashed-line boxes in Fig. 1. The events in the yellow sideband box are mainly from $\Sigma^0(1385)$ and are excluded when evaluating the other background contributions. Since there are also contributions from $\Sigma^0(1385)$ in the black box regions, the number of background events other than $\Sigma^0(1385)$ is estimated by $(N^{\text{data}}_{\text{black}} - N^{\Sigma^0(1385)}_{\text{black}})/3$, where $N^{\text{data}}_{\text{black}}$ and $N^{\Sigma^0(1385)}_{\text{black}}$ are the numbers of events in the black boxes from data and the MC simulated $\Sigma^0(1385)$ sample, respectively. Finally, the number of background events other than $\Sigma^0(1385)$ in the signal region is estimated to be 4641 ± 138. The final selected data sample has a high signal purity of (98.1 ± 0.2)%.

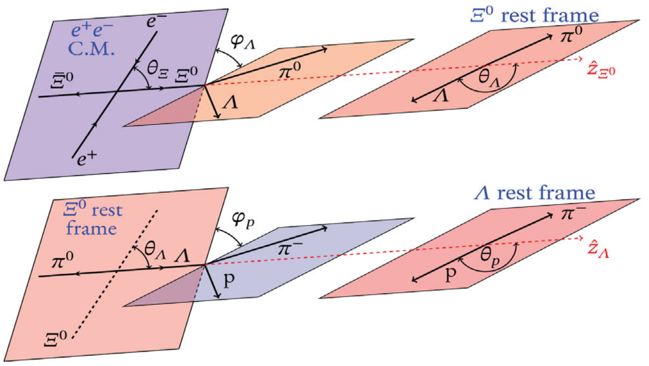

FIG. 2. Definitions of the helicity angles. The polar angle θ_Ξ is the angle between the Ξ^0 momentum and the e^+ beam direction in the e^+e^- center-of-mass system (c.m.), where the $\hat{z}$ axis is defined along the e^+ momentum. Note that θ_Λ and φ_Λ are the polar and azimuthal angles of the Λ momentum direction in the Ξ^0 rest frame, where $\hat{z}_{\Xi^0}$ is defined along the Ξ^0 momentum direction in the e^+e^- c.m., and $\hat{y}_{\Xi^0}$ is defined by $\hat{z} \times \hat{z}_{\Xi^0}$. The angles θ_p and φ_p are the polar and azimuthal angles of the proton momentum direction in the Λ rest frame, where $\hat{z}_\Lambda$ is defined along the Λ momentum in the Ξ^0 rest frame, and $\hat{y}_\Lambda$ is along $\hat{z}_{\Xi^0} \times \hat{z}_\Lambda$.

Following the formulation in Refs. [43–46], the joint angular distribution of the full decay chain is obtained, denoted as $\mathcal{W}(\vec{\omega}; \vec{\zeta})$, and the final expression is identical to the one developed by the helicity frame [22,47]. Here, $\vec{\omega}$ represents the eight parameters of interest, $\alpha_{J/\psi}$, $\Delta\Phi$, α_Ξ, $\bar{\alpha}_\Xi$, ϕ_Ξ, $\bar{\phi}_\Xi$, α_Λ, and $\bar{\alpha}_\Lambda$, where $\alpha_{J/\psi}$ and $\Delta\Phi$ are related to the psionic form factors [48] and govern the scattering angle distribution and the polarization of the Ξ^0; $\vec{\zeta}$ stands for nine angle variables, θ_Ξ, θ_Λ, φ_Λ, $\theta_{\bar{\Lambda}}$, $\varphi_{\bar{\Lambda}}$, θ_p, φ_p, $\theta_{\bar{p}}$, and $\varphi_{\bar{p}}$. These helicity angles are constructed as illustrated in Fig. 2, and the corresponding angles of the antiparticle decay sequence are obtained analogously. Detailed information about this formalism can be found in Ref. [22].

A nine-dimensional maximum likelihood fit is performed on the joint angular distribution from data to determine the eight $\vec{\omega}$ parameters, similar to that in Ref. [20]. In the fit, the events from the data sideband regions and the $\Sigma^0(1385)$ MC sample are included with a negative weight to subtract the background effects, where the likelihood function of background events is the same as the signal events. The results are summarized in Table I, together with previous measurements [20,42,49]. In this table, we also present the averaged values of the decay parameters, which are defined as $\langle\alpha_\Xi\rangle = (\alpha_\Xi - \bar{\alpha}_\Xi)/2$, $\langle\phi_\Xi\rangle = (\phi_\Xi - \bar{\phi}_\Xi)/2$, $\langle\alpha_\Lambda\rangle = (\alpha_\Lambda - \bar{\alpha}_\Lambda)/2$.

The Ξ^0 polarization can be illustrated through the moment μ, defined as

$$\mu^k(\cos\theta_\Xi) = \frac{1}{N^k}\sum_i^{N^k}(\sin\theta^i_\Lambda \sin\varphi^i_\Lambda + \sin\theta^i_{\bar{\Lambda}} \sin\varphi^i_{\bar{\Lambda}}), \tag{6}$$

TABLE I. The $J/\psi \to \Xi^0\bar{\Xi}^0$ angular distribution parameter $\alpha_{J/\psi}$; the relative phase $\Delta\Phi$ of the psionic form factors; the decay parameters for $\Xi^0 \to \Lambda\pi^0(\alpha_\Xi, \phi_\Xi)$, $\bar{\Xi}^0 \to \bar{\Lambda}\pi^0(\bar{\alpha}_\Xi, \bar{\phi}_\Xi)$, $\Lambda \to p\pi^+(\alpha_\Lambda)$, and $\bar{\Lambda} \to \bar{p}\pi^+(\bar{\alpha}_\Lambda)$; the *CP* asymmetries A^Ξ_{CP}, $\Delta\phi^\Xi_{CP}$, and A^Λ_{CP}; and the averages $\langle\alpha_\Xi\rangle$, $\langle\phi_\Xi\rangle$, and $\langle\alpha_\Lambda\rangle$. The first and second uncertainties are statistical and systematic, respectively.

Parameter	This work	Previous result
$\alpha_{J/\psi}$	$0.514 \pm 0.006 \pm 0.015$	0.66 ± 0.06 [42]
$\Delta\Phi$(rad)	$1.168 \pm 0.019 \pm 0.018$	…
α_Ξ	$-0.3750 \pm 0.0034 \pm 0.0016$	-0.358 ± 0.044 [49]
$\bar{\alpha}_\Xi$	$0.3790 \pm 0.0034 \pm 0.0021$	0.363 ± 0.043 [49]
ϕ_Ξ(rad)	$0.0051 \pm 0.0096 \pm 0.0018$	0.03 ± 0.12 [49]
$\bar{\phi}_\Xi$(rad)	$-0.0053 \pm 0.0097 \pm 0.0019$	-0.19 ± 0.13 [49]
α_Λ	$0.7551 \pm 0.0052 \pm 0.0023$	0.7519 ± 0.0043 [20]
$\bar{\alpha}_\Lambda$	$-0.7448 \pm 0.0052 \pm 0.0017$	-0.7559 ± 0.0047 [20]
$\xi_P - \xi_S$(rad)	$(0.0 \pm 1.7 \pm 0.2) \times 10^{-2}$	…
$\delta_P - \delta_S$(rad)	$(-1.3 \pm 1.7 \pm 0.4) \times 10^{-2}$	…
A^Ξ_{CP}	$(-5.4 \pm 6.5 \pm 3.1) \times 10^{-3}$	$(-0.7 \pm 8.5) \times 10^{-2}$ [49]
$\Delta\phi^\Xi_{CP}$(rad)	$(-0.1 \pm 6.9 \pm 0.9) \times 10^{-3}$	$(-7.9 \pm 8.3) \times 10^{-2}$ [49]
A^Λ_{CP}	$(6.9 \pm 5.8 \pm 1.8) \times 10^{-3}$	$(-2.5 \pm 4.8) \times 10^{-3}$ [20]
$\langle\alpha_\Xi\rangle$	$-0.3770 \pm 0.0024 \pm 0.0014$	…
$\langle\phi_\Xi\rangle$(rad)	$0.0052 \pm 0.0069 \pm 0.0016$	…
$\langle\alpha_\Lambda\rangle$	$0.7499 \pm 0.0029 \pm 0.0013$	0.7542 ± 0.0026 [20]

where N^k is the number of events in the kth $\cos\theta_\Xi$ bin and i is the ith event in that bin. The expected angular dependence of the moment for the acceptance-corrected data is given by

$$\mu(\cos\theta_\Xi) = \frac{\alpha_\Xi - \bar{\alpha}_\Xi}{2} \frac{1 + \alpha_{J/\psi}\cos^2\theta_\Xi}{3 + \alpha_{J/\psi}} P_y(\theta_\Xi), \quad (7)$$

where $P_y(\theta_\Xi) = \sqrt{1 - \alpha^2_{J/\psi}}\sin(\Delta\Phi)\cos\theta_\Xi\sin\theta_\Xi/(1 + \alpha_{J/\psi}\cos^2\theta_\Xi)$ is the polarization of Ξ^0. Comparing the data to the PHSP MC sample, as shown in Fig. 3, there is a significant polarization of the Ξ^0 hyperons produced in $J/\psi \to \Xi^0\bar{\Xi}^0$ decays, manifested in the relative phase $\Delta\Phi = 1.168 \pm 0.019_{\text{stat}} \pm 0.018_{\text{syst}}$ radians.

The systematic uncertainties can be separated into two categories: (1) the differences between data and simulation and (2) the uncertainties associated with the fit procedure.

The systematic uncertainties from $\Lambda/\bar{\Lambda}$ reconstruction, π^0 reconstruction, and the kinematic fit are studied with control samples. A control sample of $J/\psi \to pK^-\bar{\Lambda}$ + c.c. is used to estimate the uncertainties from the $\Lambda/\bar{\Lambda}$ reconstruction. The systematic uncertainties from π^0 reconstruction and the 4C kinematic fit are investigated by a control sample of $J/\psi \to \Xi^0(\to \Lambda\pi^0)\bar{\Xi}^0(\to \bar{\Lambda}\pi^0)$. The efficiency differences between data and MC for the control samples are used to reweight the PHSP MC sample. The differences between the fitting results with corrections and the nominal fitting are taken as the systematic uncertainties.

The mass window of $\Xi^0/\bar{\Xi}^0$ is $\pm 3\sigma$ around the known Ξ^0 mass, where $\sigma = 4.8$ MeV$/c^2$ is the resolution of the reconstructed $\Xi^0/\bar{\Xi}^0$ mass. We change it to $\pm 2\sigma$ or $\pm 4\sigma$ to study the systematic uncertainties from the $\Xi^0/\bar{\Xi}^0$ mass window. The fit is repeated, and the largest deviations from the nominal values are taken as the signal mass window systematic uncertainties.

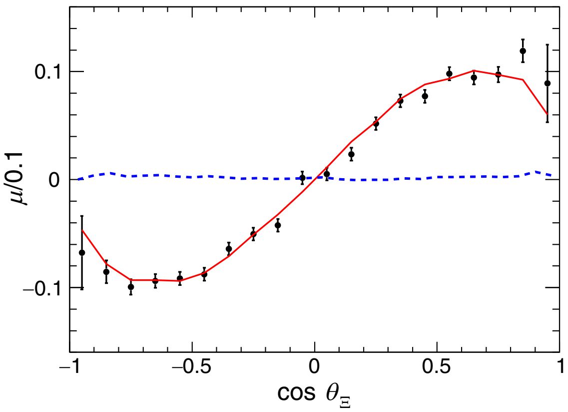

FIG. 3. Distribution of the moment $\mu(\cos\theta_\Xi)$ versus $\cos\theta_\Xi$. The points with error bars are data, the red solid lines are from the signal MC, and the blue dashed line represents the distribution without polarization from the PHSP MC sample.

TABLE II. Absolute systematic uncertainties for the measured parameters.

Source (10^{-3})	$\alpha_{J/\psi}$	$\Delta\Phi$(rad)	α_{Ξ}	$\bar{\alpha}_{\Xi}$	ϕ_{Ξ}(rad)	$\bar{\phi}_{\Xi}$(rad)	α_{Λ}	$\bar{\alpha}_{\Lambda}$	$\xi_P - \xi_S$ (rad)	$\delta_P - \delta_S$ (rad)	A_{CP}^{Ξ}	$\Delta\phi_{CP}^{\Xi}$ (rad)	A_{CP}^{Λ}	$\langle\alpha_{\Xi}\rangle$	$\langle\phi_{\Xi}\rangle$(rad)	$\langle\alpha_{\Lambda}\rangle$
$\Lambda/\bar{\Lambda}$ reconstruction	9	8	0.1	1.8	0.6	0.1	1.0	0.8	1	1	2.3	0.3	0.1	0.8	0.3	0.8
π^0 reconstruction	2	6	0.5	0.4	1.2	1.1	0.0	0.0	0	3	0.1	0.1	0.0	0.5	1.1	0.1
4C Kinematic fit	7	8	0.9	0.3	0.8	0.8	0.8	0.3	2	0	1.7	0.8	0.3	0.3	0.0	0.5
$\Xi^0/\bar{\Xi}^0$ mass window	3	7	0.5	0.0	0.0	0.0	0.0	0.0	0	0	0.0	0.0	0.0	0.4	0.0	0.0
Background estimation	0	1	0.1	0.2	0.3	0.5	0.5	0.8	0	1	0.2	0.3	0.3	0.1	0.3	0.5
$\cos\theta_{\Xi}$ inconsistency	8	9	0.9	1.0	0.6	0.5	0.7	0.8	0	2	0.1	0.1	0.0	0.9	0.5	0.7
Fit method	3	6	0.6	0.2	0.7	1.1	1.7	0.9	1	2	1.1	0.2	1.7	0.2	0.9	0.4
Total	15	18	1.6	2.1	1.8	1.9	2.3	1.7	2	4	3.1	0.9	1.8	1.4	1.6	1.3

The systematic uncertainties from the background estimation are studied by varying the estimated background yields by 1 standard deviation or changing the sideband regions from $|m_{\Lambda\pi^0}(m_{\bar{\Lambda}\pi^0}) - M_{\Xi^0}| \in [0.0285, 0.0575]$ GeV/c^2 to $|m_{\Lambda\pi^0}(m_{\bar{\Lambda}\pi^0}) - M_{\Xi^0}| \in [0.0235, 0.0525]$ GeV/c^2. The biggest differences between the results with the modified background yields and nominal ones are taken as the systematic uncertainties.

On the left and right sides ($|\cos\theta_{\Xi}| > 0.85$) of the $\cos\theta_{\Xi}$ distribution, the number of events in data is observed to be smaller than that in the MC simulations, where the total number of events of the MC sample is normalized to data. To estimate their effect on the final results, the ratios of $n^i_{\text{data}}/n^i_{\text{MC}}$ are obtained in different $\cos\theta_{\Xi}$ bins, where n^i_{data} and n^i_{MC} are the number of events in the ith $\cos\theta_{\Xi}$ bin from the data and MC sample, respectively. The ratios are then used to reweight the MC sample, and the differences between the results after weighting and the nominal results are taken as systematic uncertainties.

All the above systematic uncertainties belong to category (1); here, we consider category (2), the uncertainties caused by the fit method. This source of systematic uncertainties is estimated by analyzing the signal MC sample which is approximately 100 times our nominal data sample. The differences between the obtained parameter values and the ones we used to generate the signal MC sample are regarded as systematic uncertainties.

The absolute systematic uncertainties for various sources are summarized in Table II. The total systematic uncertainties of various parameters are obtained by summing the individual contributions in quadrature.

In summary, this Letter presents the most precise determination of all $\Xi^0 \to \Lambda\pi^0/\bar{\Xi}^0 \to \bar{\Lambda}\pi^0$ decay parameters, which are improved by more than 1 order of magnitude over the previous measurements [49], as shown in Table I. The averaged values of the Ξ^0 decay parameters are determined to be $\langle\alpha_{\Xi}\rangle = -0.3770 \pm 0.0024_{\text{stat}} \pm 0.0014_{\text{syst}}$ and $\langle\phi_{\Xi}\rangle = 0.0052 \pm 0.0069_{\text{stat}} \pm 0.0016_{\text{syst}}$ for the first time, which will be valuable inputs for many other baryon studies involving Ξ^0 decay. A clear transverse polarization of Ξ^0 from J/ψ decay is observed for the first time, and the relative phase of the psionic form factors is determined to be $\Delta\Phi = 1.168 \pm 0.019_{\text{stat}} \pm 0.018_{\text{syst}}$ rad. This result is significantly different from the $\psi(3686) \to \Xi^0\bar{\Xi}^0$ decay [49], $\Delta\Phi_{\psi(3686)} = -0.050 \pm 0.150_{\text{stat}} \pm 0.020_{\text{syst}}$, where no polarization was found. These observations will provide a key probe of the decay dynamics on the charmonium decays to hyperon pairs. The *CP* asymmetry observables are measured to be $A^{\Xi}_{CP} = (-5.4 \pm 6.5_{\text{stat}} \pm 3.1_{\text{syst}}) \times 10^{-3}$ and $\Delta\phi^{\Xi}_{CP} = (-0.1 \pm 6.9_{\text{stat}} \pm 0.9_{\text{syst}}) \times 10^{-3}$ with the highest precision to date. We find *CP* symmetry is conserved in the Ξ^0 decay with an accuracy of 10^{-3}, which is in agreement with the Standard Model predictions [24]. Furthermore, the weak and strong phase differences in Ξ^0 decay, $\xi_P - \xi_S = (0.0 \pm 1.7_{\text{stat}} \pm 0.2_{\text{syst}}) \times 10^{-2}$ and $\delta_P - \delta_S = (-1.3 \pm 1.7_{\text{stat}} \pm 0.4_{\text{syst}}) \times 10^{-2}$, are directly measured for the first time. These are the most precise results for any weakly decaying baryon, and they are crucial for understanding *CP* violation sources beyond the Standard Model. At the same time, the decay parameters and *CP* asymmetry observable of the decay $\Lambda \to p\pi^-/\bar{\Lambda} \to \bar{p}\pi^+$ are determined. The parameter α_{Λ} is found to be in excellent agreement with the determinations from $J/\psi \to \Lambda\bar{\Lambda}$ and $J/\psi \to \Xi^-\bar{\Xi}^+$ samples [20,22] but in 3.5σ tension with the CLAS result, $0.721 \pm 0.006_{\text{stat}} \pm 0.005_{\text{syst}}$ [50]. With the properties of the quantum-entangled hyperon-antihyperon, the proposed, future, super tau-charm factories [51,52] may have the potential to discover *CPV* in the baryon sector.

The BESIII Collaboration thanks the staff of BEPCII and the IHEP computing center for their strong support. This work is supported in part by the National Key R&D Program of China under Contracts No. 2020YFA0406300 and No. 2020YFA0406400; the National Natural Science Foundation of China (NSFC) under Contracts No. 11635010, No. 11735014, No. 11835012, No. 11935015, No. 11935016, No. 11935018, No. 11961141012, No. 12022510, No. 12025502, No. 12035009, No. 12035013, No. 12061131003, No. 12192260, No. 12192261, No. 12192262, No. 12192263, No. 12192264, No. 12192265, No. 12221005, No. 12225509, and No. 12235017; the Chinese Academy of Sciences (CAS) Large-Scale Scientific Facility Program; the CAS Center for Excellence in Particle Physics (CCEPP); the CAS Key Research Program of Frontier Sciences under Contracts No. QYZDJ-SSW-SLH003 and No. QYZDJ-SSW-SLH040; 100 Talents Program of CAS; the Institute of Nuclear and Particle Physics (INPAC) and Shanghai Key Laboratory for Particle Physics and Cosmology; the ERC under Contract No. 758462; European Union's Horizon 2020 research and innovation program under Marie Sklodowska-Curie grant agreement under Contract No. 894790; the German Research Foundation DFG under Contracts No. 443159800 and No. 455635585, and Collaborative Research Center CRC 1044, FOR5327, GRK 2149; Olle Engkvist Foundation, Contract No. 200-0605; Lundström-Åman Foundation; Knut and Alice Wallenberg Foundation, Contracts No. 2016.0157 and No. 2021.0299; Swedish Research Council, Contracts No. 2019-04594 and No. 2021-04567; Swedish Foundation for International Cooperation in Research and Higher Education, Contract No. CH2018-7756; Istituto Nazionale di Fisica Nucleare, Italy; Ministry of Development of Turkey under Contract No. DPT2006K-120470; National Research Foundation of Korea under Contract No. NRF-2022R1A2C1092335; National Science and Technology fund of Mongolia; National Science Research and Innovation Fund (NSRF) via the Program Management Unit for Human Resources & Institutional Development, Research and Innovation of Thailand under Contract No. B16F640076; Polish National Science Centre under Contract No. 2019/35/O/ST2/02907; the Swedish Research Council; the U.S. Department of Energy under Contract No. DE-FG02-05ER41374.

[1] A. D. Sakharov, Pis'ma Zh. Eksp. Teor. Fiz. **5**, 32 (1967).

[2] J. H. Christenson, J. W. Cronin, V. L. Fitch, and R. Turlay, Phys. Rev. Lett. **13**, 138 (1964).

[3] B. Aubert *et al.* (*BABAR* Collaboration), Phys. Rev. Lett. **87**, 091801 (2001).

[4] K. Abe *et al.* (Belle Collaboration), Phys. Rev. Lett. **87**, 091802 (2001).

[5] R. Aaij *et al.* (LHCb Collaboration), Phys. Rev. Lett. **122**, 211803 (2019).

[6] W. Bernreuther, Lect. Notes Phys. **591**, 237 (2002).

[7] L. Canetti, M. Drewes, and M. Shaposhnikov, New J. Phys. **14**, 095012 (2012).

[8] J. F. Donoghue and S. Pakvasa, Phys. Rev. Lett. **55**, 162 (1985).

[9] J. F. Donoghue, X. G. He, and S. Pakvasa, Phys. Rev. D **34**, 833 (1986).

[10] N. Salone, P. Adlarson, V. Batozskaya, A. Kupsc, S. Leupold, and J. Tandean, Phys. Rev. D **105**, 116022 (2022).

[11] H. B. Li, Front. Phys. (Beijing) **12**, 121301 (2017); **14**, 64001(E) (2019).

[12] M. A. Shifman, A. I. Vainshtein, and V. I. Zakharov, Nucl. Phys. **B120**, 316 (1977).

[13] F. J. Gilman and M. B. Wise, Phys. Lett. **93B**, 129 (1980).

[14] S. Weinberg, Phys. Rev. Lett. **37**, 657 (1976).

[15] T. D. Lee, Phys. Rev. D **8**, 1226 (1973).

[16] R. N. Mohapatra and J. C. Pati, Phys. Rev. D **11**, 566 (1975).

[17] G. C. Branco, J. M. Frere, and J. M. Gerard, Nucl. Phys. **B221**, 317 (1983).

[18] G. Beall and A. Soni, Phys. Rev. Lett. **47**, 552 (1981).

[19] BESIII Collaboration, Nat. Phys. **15**, 631 (2019).

[20] M. Ablikim *et al.* (BESIII Collaboration), Phys. Rev. Lett. **129**, 131801 (2022).

[21] M. Ablikim *et al.* (BESIII Collaboration), Phys. Rev. Lett. **125**, 052004 (2020).

[22] M. Ablikim *et al.* (BESIII Collaboration), Nature (London) **606**, 64 (2022).

[23] M. Ablikim *et al.* (BESIII Collaboration), Phys. Rev. D **106**, L091101 (2022).

[24] X. G. He, J. Tandean, and G. Valencia, Sci. Bull. **67**, 1840 (2022).

[25] T. D. Lee and C. N. Yang, Phys. Rev. **108**, 1645 (1957).

[26] M. Bourquin *et al.* (BRISTOL-GENEVA-HEIDELBERG-ORSAY-RUTHERFORD-STRASBOURG Collaboration), Nucl. Phys. **B241**, 1 (1984).

[27] J. M. Link *et al.* (FOCUS Collaboration), Phys. Lett. B **634**, 165 (2006).

[28] T. Z. Han, R. G. Ping, T. Luo, and G. Z. Xu, Chin. Phys. C **44**, 013002 (2020).

[29] M. Ablikim *et al.* (BESIII Collaboration), Chin. Phys. C **46**, 074001 (2022).

[30] C. Yu *et al.*, *Proceedings of IPAC2016, Busan, Korea* (2016), 10.18429/JACoW-IPAC2016-TUYA01.

[31] M. Ablikim *et al.*, Nucl. Instrum. Methods Phys. Res., Sect. A **614**, 345 (2010).

[32] M. Ablikim *et al.* (BESIII Collaboration), Chin. Phys. C **44**, 040001 (2020).

[33] K. X. Huang, Z. J. Li, Z. Qian, J. Zhu, H. Y. Li, Y. M. Zhang, S. S. Sun, and Z. Y. You, Nucl. Sci. Tech. **33**, 142 (2022).

[34] S. Agostinelli *et al.* (GEANT4 Collaboration), Nucl. Instrum. Methods Phys. Res., Sect. A **506**, 250 (2003).

[35] Z. Y. Deng *et al.*, Chin. Phys. C **30**, 371 (2006), http://cpc.ihep.ac.cn/article/id/283d17c0-e8fa-4ad7-bfe3-92095466def1.

[36] S. Jadach, B. F. L. Ward, and Z. Was, Phys. Rev. D **63**, 113009 (2001).

[37] D. J. Lange, Nucl. Instrum. Methods Phys. Res., Sect. A **462**, 152 (2001); R. G. Ping, Chin. Phys. C **32**, 599 (2008).

[38] J. C. Chen, G. S. Huang, X. R. Qi, D. H. Zhang, and Y. S. Zhu, Phys. Rev. D **62**, 034003 (2000); R. L. Yang,

R. G. Ping, and H. Chen, Chin. Phys. Lett. **31**, 061301 (2014).

[39] M. Xu *et al.*, Chin. Phys. C **33**, 428 (2009).

[40] L. Yan *et al.*, Chin. Phys. C **34**, 204 (2010).

[41] R. L. Workman *et al.* (Particle Data Group), Prog. Theor. Exp. Phys. **2022**, 083C01 (2022).

[42] M. Ablikim *et al.* (BESIII Collaboration), Phys. Lett. B **770**, 217 (2017).

[43] A. Z. Dubnickova, S. Dubnicka, and M. P. Rekalo, Nuovo Cimento A **109**, 241 (1996).

[44] G. I. Gakh and E. Tomasi-Gustafsson, Nucl. Phys. **A771**, 169 (2006).

[45] H. Czyz, A. Grzelinska, and J. H. Kuhn, Phys. Rev. D **75**, 074026 (2007).

[46] E. D. Commins and P. H. Bucksbaum, *Weak Interactions of Leptons and Quarks* (Addison-Wesley, Reading, MA, 1983), ISBN 978-0-521-27370-1.

[47] E. Perotti, G. Fäldt, A. Kupsc, S. Leupold, and J. J. Song, Phys. Rev. D **99**, 056008 (2019).

[48] G. Fäldt and A. Kupsc, Phys. Lett. B **772**, 16 (2017).

[49] M. Ablikim *et al.* (BESIII Collaboration), Phys. Rev. D **108**, L011101 (2023).

[50] D. G. Ireland, M. Döring, D. I. Glazier, J. Haidenbauer, M. Mai, R. Murray Smith, and D. Rönchen, Phys. Rev. Lett. **123**, 182301 (2019).

[51] A. E. Bondar, Phys. At. Nucl. **76**, 1072 (2013).

[52] M. Achasov *et al.*, arXiv:2303.15790.